



*Asesorías y Tutorías para la Investigación Científica en la Educación Puig-Salabarría S.C.
José María Pino Suárez 400-2 esq a Lerdo de Tejada, Toluca, Estado de México. 7223898475*

RFC: ATII20618V12

Revista Dilemas Contemporáneos: Educación, Política y Valores.

<http://www.dilemascontemporaneoseducacionpoliticayvalores.com/>

Año: VI

Número: Edición Especial

Artículo no.:71

Período: Marzo, 2019.

TÍTULO: Aplicación del filtro de paso bajo (LPF) basado en el amplificador operacional de transconductancia (OTA).

AUTORES:

1. Ridouane Hamdaouy.
2. Mostapha Boussetta.
3. Khadija Slaoui.

RESUMEN. Este artículo presenta el diseño del filtro de paso bajo de primer orden utilizando el amplificador operacional de transconductancia (OTA). Este documento ilustra una aplicación de OTA como un filtro de paso bajo activo. El bloque de construcción principal de una OTA es el espejo actual. Se utilizan diferentes réplicas actuales para diseñar el LPF y las respuestas de frecuencia y fase correspondientes se estudian de manera comparativa en este documento. Con OOS de CMOS OTA y NMOS de OTA de NMOS comparativos se estudiarán pero también se ilustran en este artículo.

PALABRAS CLAVES: Amplificador operacional de transconductancia, CMOS OTA, NMOS OTA, filtro.

TITLE: Application of the operational transconductance amplifier (OTA) based low pass filter (LPF).

AUTHORS:

1. Ridouane Hamdaouy
2. Mostapha Boussetta
3. Khadija Slaoui

ABSTRACT: This paper presents designing of first order low pass filter using Operational Transconductance Amplifier (OTA). This paper illustrates an application of OTA as an active low pass filter. The primary building block of an OTA is the current mirror. Different current mirrors are used to design the LPF & the corresponding frequency and phase responses are comparatively studied in this paper. With comparatively CMOS OTA & NMOS OTA are to study but also illustrated in this article.

KEY WORDS: Operational Transconductance Amplifier, CMOS OTA, NMOS OTA, filter.

INTRODUCTION.

For analog signal processing, a wide range of the active devices are easily available in the literature. The analog signal processing devices can be classified into two groups such as voltage mode and current mode devices. Formerly, voltage mode active blocks such as op-amps were widely used. In terms of bandwidth, slew rate, power dissipation and circuit complexity, the voltage mode devices exhibit the worse performance. Therefore, the current mode devices such as current conveyors and operational transconductance amplifiers (OTA) have become more popular in recent years.

The operational transconductance amplifier (OTA) is basically an op-amp without output buffer. The bias voltage in an OTA controls the bias current flowing through the current mirror circuit, which in turns affects the “ g_m ”. All the standard filter parameters of interest are directly proportional to “ g_m ” of the OTA. Furthermore, the OTAs produce output current proportional to the differential input voltage and their gain can be controlled by the bias current. Thus, the OTAs are

useful devices for current controlled applications. Active filter widely applied in the field of electrical engineering. They can be found in cross over network used in a three-way high-fidelity loud speaker, portable ECG detection used in front end circuits and touch-tone telephone used for tone decoding. Several active devices were used to realize tunable active filters, i.e. OTA, OP-AMP, CDTA, Second generation current-controlled current conveyor. OTA is widely used to realize linear and non-linear Analog signal processing circuits. It is well known that an OTA provides an electronic tenability, a wide range of its transconductance gain and simple circuitry. Furthermore, OTA-based circuits require no resistors hence they are highly suitable for IC implementation.

In the rapid development of the wireless communication field, the transceiver system with high performance is a hot research area in recent years (Acosta, Jiménez, Ramón, Carvajal, 2009). The filter is one of the most important part in this system, is the key module to solve transceiver performance, with low cost and low power CMOS technology to increase the feasibility of the design of high-performance filter. So, it is very important to design a low power and high-performance filter with low power consumption. An active low pass filter is an analog circuit that is widely used in communication systems and signal processing to pass a range of frequencies and reject the higher frequency (Hsu, Ho, Wu and Chen, 2006).

It can be easily designed by a conventional operational amplifier. But CMOS operational transconductance amplifier can be used to design an LPF resulting reduced power dissipation & fabrication cost (Hsu, Ho, Wu and Chen, 2006; Villegas, Casson, and Corbishley 2011; Liu, Peng and Wu, 2009; Mahapatra, Singh, and Kumar, 2009; Geiger and Sánchez-Sinencio, 1985). Some earlier works are enlisted in the references (Malvar, 1982; Waldman, García, González, and Cordero, 2018; Timar and Rencz, 2007; Solis-Bustos, et al. 2000; salman & Borkar, 2016). where CMOS OTA is used. But in this work, we have started our work with NMOS OTA with different

current mirror load. The proposed OTA and the low pass filter are simulated with 0.13 μ m CMOS technology parameters using cadence virtuoso. The proposed circuit can operate with 3.3 V and consume low power. Also, the circuit not only exhibits good slew rate performance but also has an acceptable frequency behavior. Then we have designed the LPF by CMOS OTA with different current mirror loads. As a result, a comparative study has been concluded that CMOS OTA is much more important than NMOS OTA in designing analog circuits.

DEVELOPMENT.

Theory and principles.

A. Basic Concept of OTA.

The difference between an Operational Amplifier (OpAmp) and an Operational Transconductance Amplifier (OTA) is that the op-amp has got an output buffer so that it is able to drive resistive loads. An OTA can only drive capacitive loads. Design of OTA is very important to get accurate filter results.

The OTA is characterized by various parameters like PSRR (dB), Slew Rate (SR), CMRR dB (dB), Output Offset Voltage (Vof). All the sources are connected to their bulk reducing the body bias effect to zero. For the maximum gain to achieve, all the transistors are made to work in saturation region.

An OTA is a voltage controlled current source, more specifically the term “operational” comes from the fact that it takes the difference of two voltages as the input for the output current conversion. The ideal transfer characteristic is therefore, $I_{out}=g_m/(V_{in+}-V_{in-})$ where V_{in+} =Input voltage applied at the non-inverting input terminal of the OTA, V_{in-} =Input voltage applied at the inverting input terminal of the OTA and g_m =Transconductance of the OTA. An ideal OTA has two voltage inputs with infinite impedance (i.e. there is no input current). In reality, the transconductance is also a function of the input differential voltage and dependent on temperature.

The common mode input range is also infinite, while the differential signal between these two inputs is used to control an ideal current source (i.e. the output current does not depend on the output voltage) that functions as an output. The proportionality factor between output current and input differential voltage is called transconductance. The term "transconductance" comes about because the ratio of the output current over the input voltage, g_m , has the unit of a conductance if looked at "across the amplifier". Fig. 1, Fig. 2 and Fig. 3 show the macro model, ideal model and small signal equivalent model of OTA respectively.

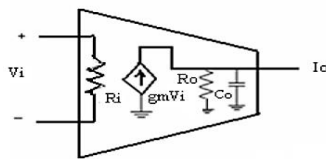


Fig. 1 Macro model of OTA.

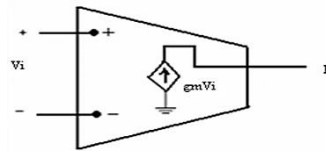


Fig. 2 Ideal model of OTA.

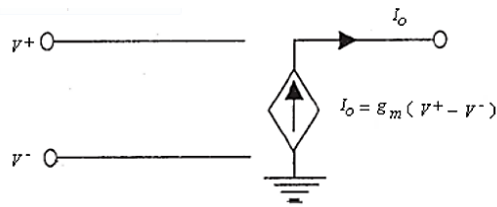


Fig. 3 Small signal equivalent model of OTA.

The amplifier's output voltage is the product of its output current and its load resistance:

$$V_{out} = R_{LOAD} * I_{out} \quad (1)$$

The voltage gain is then the output voltage divided by the differential input voltage:

$$G_m = V_{out} / (V_{in+} - V_{in-}) \quad (2)$$

The proportional factor of output vs. input for an amplifier with current input and voltage output has the unit of a resistance and such an amplifier is called a transresistance amplifier.

Current Mirror Fundamentals.

An OTA is basically a differential amplifier with active current mirror load to accomplish high gain. As the name itself suggests a current mirror is used to generate a replica (if necessary, it may be attenuated or amplified) of a given reference current. If we look at the electric function of the circuit, a current mirror is a current controlled current source (CCCS). A current mirror is basically nothing more than a current amplifier. The ideal characteristics of a current amplifier are:

- Output current linearly related to the input current, $I_{out} = A_i \cdot I_{ref}$
- Input resistance is zero
- Output resistance is infinity
- Large short-circuit current gain

In addition, we have the characteristic V_{min} which applies not only to the output but also the input. $V_{min}(in)$ is the range of input voltage over which the input resistance is not small and $V_{min}(out)$ is the range of the output voltage over which the output resistance is not large.

Fig. 4, Fig. 5 and Fig. 6 show the block diagram, transfer characteristics and output characteristics of a current mirror respectively.

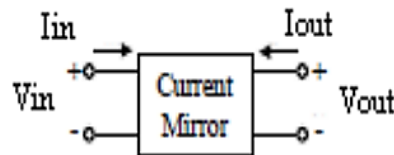


Fig. 4 Block diagram of current mirror.

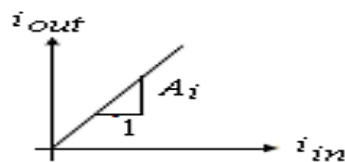
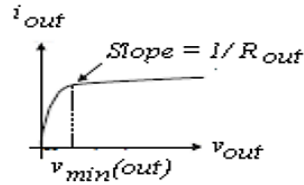


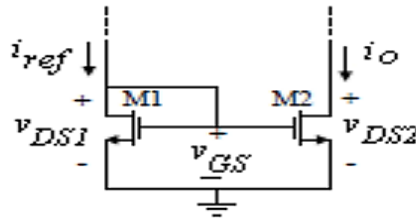
Fig. 5 Transfer characteristics of current mirror.**Fig. 6 Output characteristics of current mirror.**

Therefore, we will focus on R_{out} , R_{in} , $V_{min} (out)$, $V_{min} (in)$, and A_i to characterize the current mirror. We can design a number of circuits which can accomplish the current mirror function. The ones mostly used are.

1. Simple Current Mirror
2. Wilson Current Mirror
3. Cascade Current Mirror

Simple current mirror (Widlar): It is composed of two transistors of which one M1 is diode connected. M1 receives the reference current I_{ref} and measures it by developing at its gate the voltage V_{gs1} . This voltage biases the gate voltage of M2.

Fig. 7 below shows the schematic circuit diagram of a simple current mirror.

**Fig.7 Schematic circuit diagram of simple current mirror.**

We assume that $V_{DS2} > V_{GS2} - V_{T2}$ then,

$$\frac{i_{out}}{i_{ref}} = \left(\frac{L_1 W_2}{L_2 W_1} \right) \left(\frac{V_{GS} - V_{T2}}{V_{GS} - V_{T1}} \right)^2 \left(\frac{1 + \lambda V_{DS2}}{1 + \lambda V_{DS1}} \right) \left(\frac{K_2}{K_1} \right) \quad (3)$$

If the transistors are matched, then $K_1 = K_2$ and $V_{T1} = V_{T2}$ to give:

$$\frac{i_{out}}{i_{ref}} = \left(\frac{L_1 W_2}{L_2 W_1} \right) \left(\frac{1 + \lambda V_{DS2}}{1 + \lambda V_{DS1}} \right) \quad (4)$$

If $V_{DS1}=V_{DS2}$ then, we have

$$\frac{i_{out}}{i_{ref}} = \left(\frac{L_1 W_2}{L_2 W_1} \right) \quad (5)$$

Therefore, the sources of errors are:

- 1) V_{DS1} and V_{DS2} are not equal.
- 2) $M1$ and $M2$ are not matched.
- 3) Channel length modulation (λ) and threshold offset.

Fig. 8 shows the small signal equivalent model of a simple current mirror.

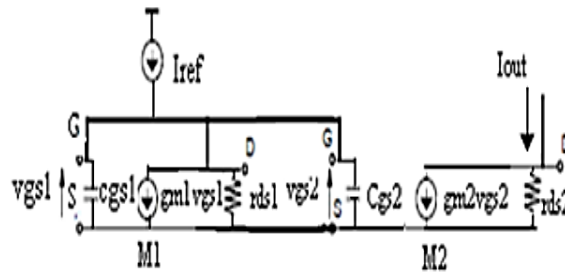


Fig.8 Small signal equivalent model of simple current mirror.

Finally,

$$\frac{i_{out}}{i_{ref}} = \frac{g_{m2}/g_{m1}}{1 + \frac{S(C_{gs1} + C_{gs2})}{g_{m1}}} \quad (6)$$

Wilson current mirror: The relatively low value of the output resistance of the simple current mirror can be improved with the Wilson scheme shown in the figure.9. The gate to source voltage $M1$ to $M2$ is equal, therefore ensuring similar operation to the circuit. However, we see that the addition of $M3$ and the established local feedback allow us to increase the output resistance.

Fig. 9 below shows the schematic circuit diagram of a Wilson current mirror.

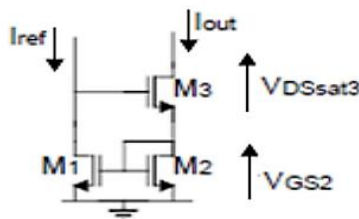


Fig.9 Schematic circuit diagram of Wilson current mirror.

Here, $V_{GS1}=V_{GS2}$, so I_{D1} is almost equal to I_{D2} .

Then,

$$\frac{i_{out}}{i_{ref}} = \left(\frac{1+\lambda V_{DS2}}{1+\lambda V_{DS1}} \right) \left(\frac{\left(\frac{W_1}{L_1}\right)}{\left(\frac{W_2}{L_2}\right)} \right) \quad (7)$$

Since,

$$V_{DS1} = V_{DS2} + V_{GS3}$$

$$\frac{i_{out}}{i_{ref}} = \left(\frac{1+\lambda V_{DS2}}{1+\lambda(V_{DS2}+V_{GS3})} \right) \left(\frac{\left(\frac{W_1}{L_1}\right)}{\left(\frac{W_2}{L_2}\right)} \right) \quad (8)$$

The output voltage swing is limited to

$$V_{out.min} = V_{GS2} + V_{DSsat.3} > V_{Th} + 2V_{DSsat} \quad (9)$$

It uses negative series feedback (M3) to achieve higher output resistance. Fig. 10 shows the small signal equivalent model of a Wilson current mirror.

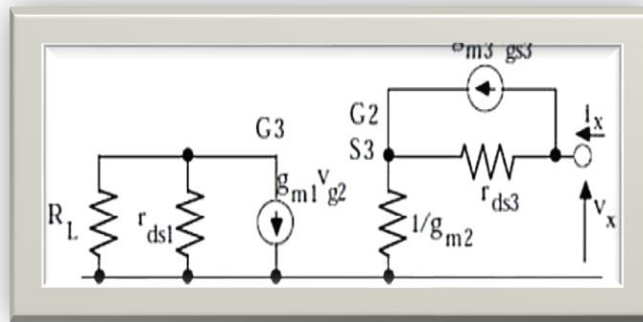


Fig. 10 Small signal equivalent model of Wilson current mirror.

Cascode current mirror:

Fig. 11 below shows the schematic circuit

diagram of a cascode

current mirror.

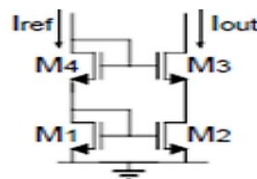


Fig.11 Schematic circuit diagram of cascode current mirror.

An alternative way to increase the output resistance is to use the cascode configuration. The output stage consists of two transistors M2, M3 in the cascode arrangement. They are biased from two other transistors M1, M4 which are diode connected. Again, as for the previously started current mirror the V_{GS} voltage of M1 and M2 are set equal. Therefore, a replica of current in M1 is generated by M2. The output resistance increases because of the cascode arrangement. Here,

$$V_{out.min} = V_{DS2} + V_{GS3} - V_{GS4} \quad (10)$$

If

$$V_{GS3} = V_{GS4}$$

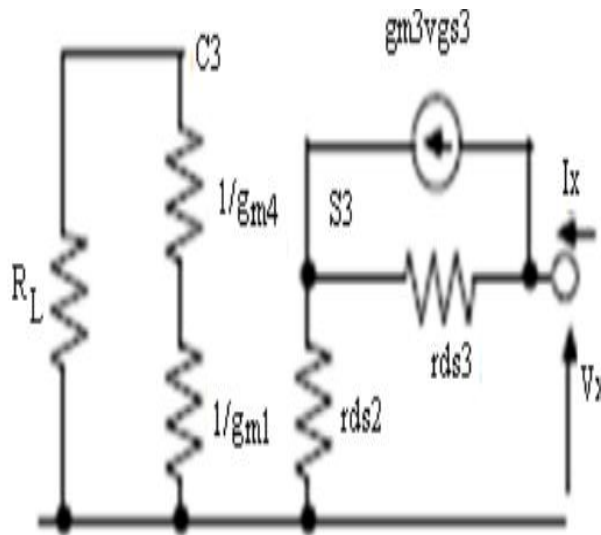
Then,

$$V_{DS1} = V_{DS2}.$$

Finally,

$$\frac{i_{out}}{i_{ref}} = \left(\frac{\frac{W_1}{L_1}}{\frac{W_2}{L_2}} \right) \quad (11)$$

Fig. 12 below shows the small signal equivalent model of a cascode current mirror.

**Fig.12.Small signal equivalent model of cascode current mirror.**

The output swing is limited to:

$$V_{out.min} = V_{GS1} + V_{GS4} - V_{GS3} + V_{DSsat3} \quad (12)$$

$$V_{out.min} = V_{GS2} + V_{DSsat.3} > V_{Th} + 2V_{DSsat}$$

Hence, the output resistance is increased without feedback.

B. NMOS OTA Design with Current Mirror Loads

When a MOSFET is using as an amplifier, input signal is given through gate terminal of the MOSFET. The bulk is tied to the bias voltage. This technique is called gate-driven in which output current is a function of input gate-to-source voltage.

NMOS OTA Design with Current Mirror Loads Fig. 13, Fig. 14 and Fig. 15 show the circuit diagram of NMOS OTA with simple, Wilson and cascode current mirror loads respectively.

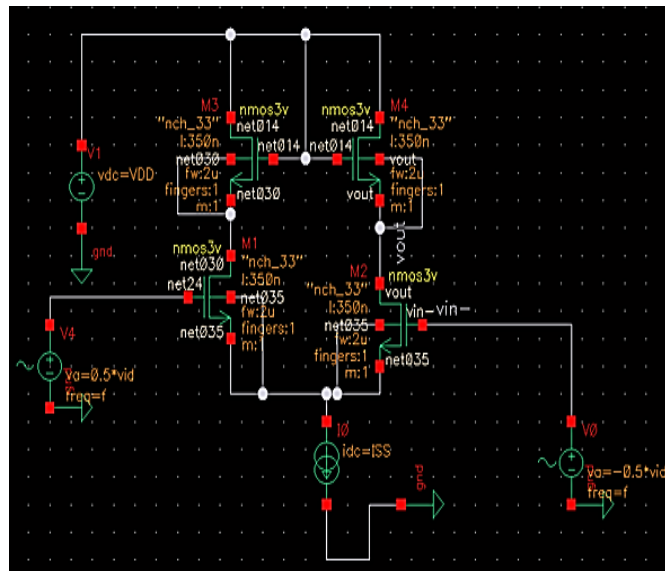


Fig13. Circuit diagram of NMOS OTA with simple current mirror load.

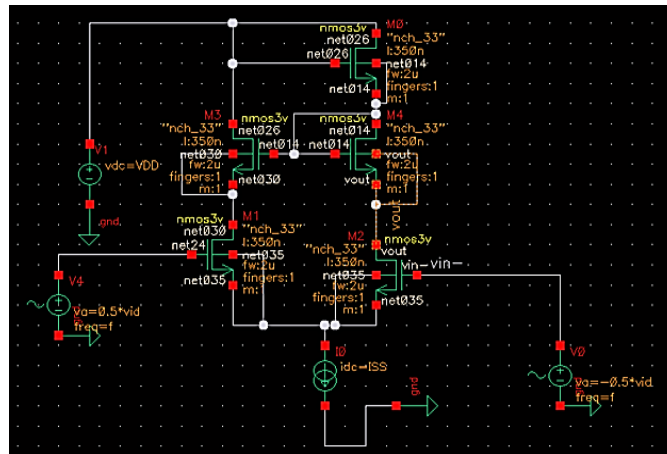


Fig.14 Circuit diagram of NMOS OTA with Wilson current mirror load.

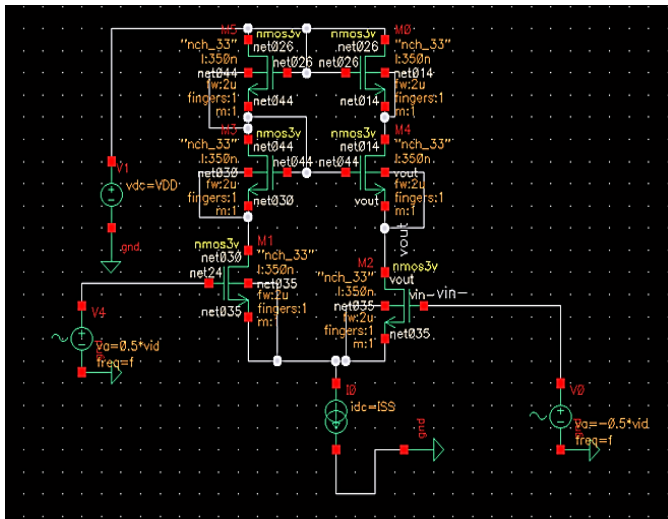


Fig.15 Circuit diagram of NMOS OTA with cascode current mirror load.

Principle of operation (simple current mirror load) The gate modifies the current through transistor in saturation term.

It shows that only one term is active at a time either gate.

In NMOS OTA the M1 and M2 transistors are operated in saturation region i.e. they satisfy the equations:

$$V_{DS1} > V_{GS1} - V_{Th1} \text{ and } V_{DS2} > V_{GS2} - V_{Th2} \quad (13)$$

The current equations are:

$$I_{D1}=0.5k_{n1}(V_{GS1}-V_{Th1})^2 \quad (14)$$

$$I_{D2}=0.5k_{n2}(V_{GS2}-V_{Th2})^2 \quad (15)$$

The sink current,

$$I_{SS}=I_{D1} + I_{D2} \quad (16)$$

M1 and M2 are assumed to be perfectly matched i.e. $K_{n1}=K_{n2}$ and $V_{Th1}=V_{Th2}$. Two cases may be possible.

Case 1: If $V_{GS1}>V_{GS2}$, then I_{D1} increases with respect to I_{D2} since $I_{SS}=I_{D1} + I_{D2}$. This increase in I_{D1} implies

increase in I_{D3} and I_{D4} . However, I_{D2} decreases when V_{GS1} is greater than V_{GS2} . Therefore, the only way to establish circuit equilibrium is for I_{out} to become positive and V_{out} decreases.

Case 2: If $V_{GS2}>V_{GS1}$, the accordingly it can be seen that I_{out} becomes negative and V_{out} increases. In this way a differential voltage is converted to output current and hence the name “operational transconductance amplifier” is justified. Other configurations of NMOS OTA can also be explained accordingly. Fig. 16 shows the small signal equivalent model of NMOS OTA with simple current mirror load.

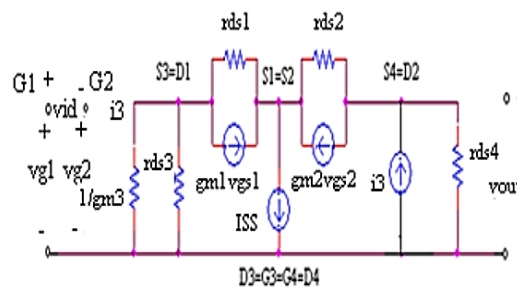


Fig.16 Small signal equivalent model of NMOS OTA with simple current mirror load.

An OTA is a voltage controlled current source device (VCCS) because in this output current is function of input voltage as shown in Figs. 13,14 and 15. Therefore the transfer function of the device is a transconductance denoted by G_m .

Limitations of NMOS OTA:

- Power dissipation is high.
- Bandwidth is less.
- Noise Margin is low.
- CMRR is low.
- Slew rate is low.
- Fabrication cost is high
- Transconductance is low.

C. CMOS OTA Design with Current Mirror Loads.

CMOS is an electronic device with high noise immunity and low static power consumption. CMOS also allows a high density of logic functions on a chip. It was primarily for this reason that CMOS became the most used technology to be implemented in VLSI chips. Here the P Channel MOSFETs of the current mirror along with the N Channel MOSFETs of the driver circuit constitute the CMOS Operational Transconductance Amplifier. We obtained different parameters like Output offset voltage, CMRR, Slew Rate, frequency response, unity gain bandwidth using different current mirrors.

A new CMOS OTA structure is presented which offers both a large differential input voltage capability and a wide g_m adjustment range. The best suited component for design of OTA is CMOS devices as it has the following advantages:

- Very less power dissipation as the feature size of CMOS processes reduce.
- CMOS provides the highest analog-to-digital on chip integration.
- Overall fabrication cost is less.
- Noise margin is high and stability performance is better.

- CMRR, Slew rate, and PSRR are improved.
- Switching speed is very high.

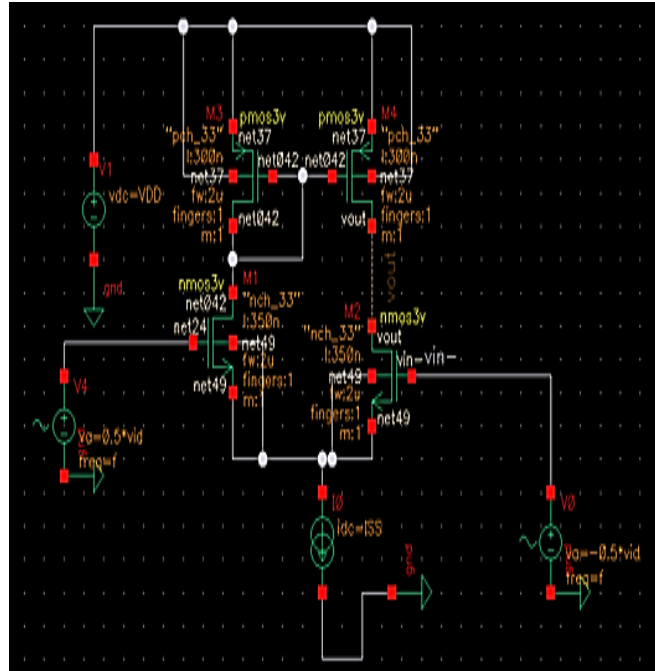


Fig .17 Circuit diagram of CMOS OTA with simple current mirror load.

Since there is existence of constant current source practically, so we have used a NMOS with $V_{gs}=V_{ds}$ while replaced the current source (ISS) such that the NMOS is in saturation. This acts as a constant current source as the current through the NMOS is constant and independent of the voltage across it.

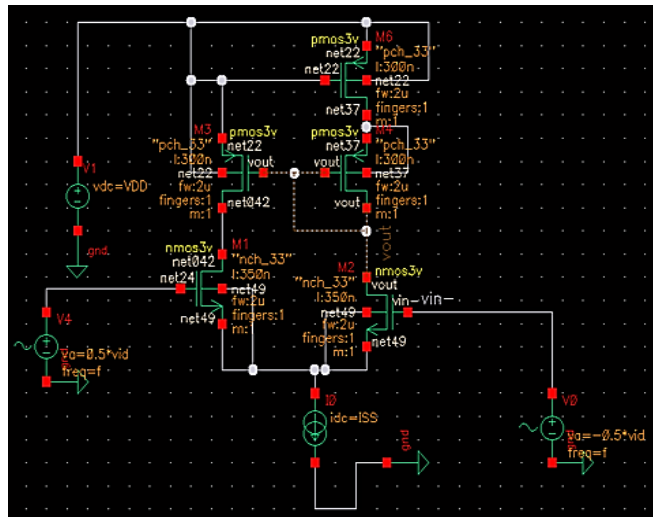


Fig .18 Circuit diagram of CMOS OTA with Wilson current mirror load.

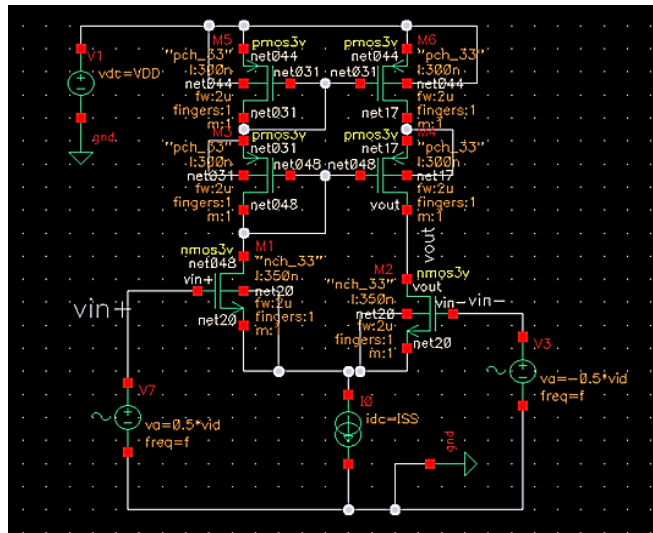


Fig. 19 Circuit diagram of CMOS OTA with cascade current mirror load.

The cascade current mirror load helps to provide high d.c gain due to its high output impedance and also remove the problem of offset voltage requirement. Moreover, this cascode current mirror load helps to increase the open loop gain of the device. Techniques implemented in the depicted OTA are namely DC biasing technique, current mirror and gate driven technique. It is a dual input and single output OTA. Inputs $V_{IN1}=vin+$ and $V_{IN2}=vin-$ are provided across transistor M1 and M2 respectively. The total number of transistors used in the said OTA is between 4 and 6. In CMOS OTA the differential amplifier part is exactly same as NMOS OTA, consisting of two NMOS

enhancement mode transistors. But the current mirror part (I-V conversion) is made of PMOS enhancement mode transistors as shown in the following figures. Figs. 17, 18 and 19 show the circuit diagram of CMOS OTA with simple, Wilson and cascode current mirror loads respectively. Fig. 20 below shows the small signal equivalent model of CMOS OTA with simple current mirror load.

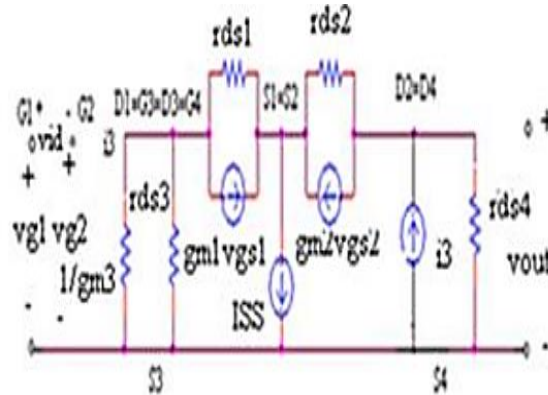


Fig. 20. Small signal equivalent model of CMOS OTA with simple current mirror load.

OTAs are used for large gain and large bandwidth performances in filters. Simple OTA also works with low power consumption and introduces very low noise in the circuit.

D. Low Pass Filter Fundamentals

A filter is a device that passes electric signals at certain frequencies or frequency ranges while preventing the passage of others. The active filters differ from passive filters (simple RC circuits) by the fact that there is the ability for gain depending on the configuration of the elements in the circuit. It consists of active elements like BJT, Opamp, FET, and MOSFET. In our design we have used NMOS OTA & CMOS OTA to design an active Low Pass Filter (LPF). The low pass filter is one that allows low frequencies to pass and stops (attenuates) higher frequencies. The design of a low pass filter needs to take into consideration the maximum frequency that would need to be allowed through. This is called the cut off frequency (or the 3dB down frequency). Based on the type of filter that is used (e.g. Butterworth, Bessel etc.) the attenuation of the higher frequencies can

be greater. This attenuation is also based on the order (e.g. 1st, 2nd, 3rd...) of the filter that is used. Based on the order of the filter the roll-off of the filter can be calculated using the formula $-n*20$ dB/decade. This means that a first order low pass filter has an attenuation of -20 dB/decade, while a second order filter should have -40 dB/decade roll-off and on down the list for higher orders. Fig. 21 shows the typical frequency response curves of low pass filter for different orders.

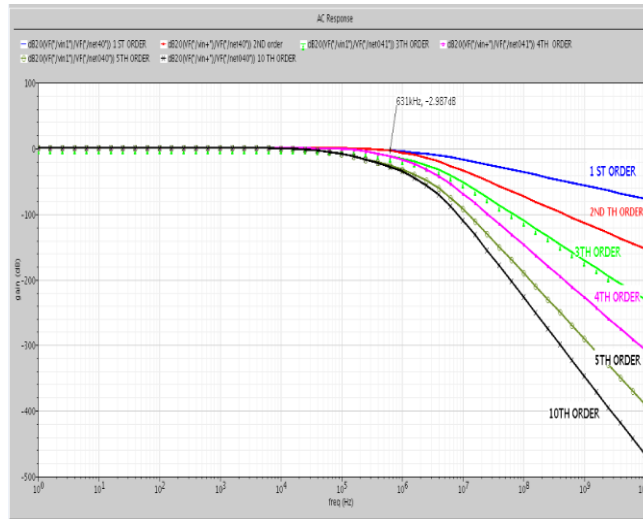


Fig. 21 Frequency response curves of low pass filter.

Proposed 1st order LPF design by NMOS and CMOS OTA.

Although low-pass filters are vital in modern electronics, their design and verification can be tedious and time consuming. An ideal low-pass filter would completely eliminate signals above the cutoff frequency, and perfectly pass signals below cutoff (in the pass-band). In real filters, various trade-offs are made in an attempt to approximate the ideal. Some filter types are optimized for gain flatness in the pass-band, some trade-off gain variation (ripple) in the pass-band for steeper roll-off, still others trade-off both flatness and rate of roll-off in favor of pulse-response fidelity.

Fig. 22 shows the circuit diagram of our proposed low pass filter by OTA.

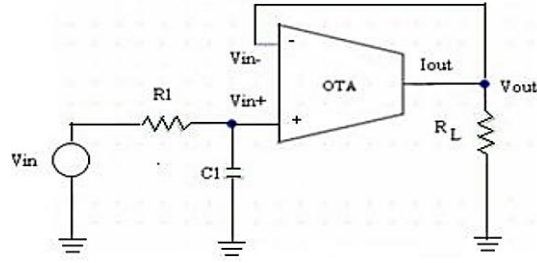


Fig. 22 Circuit diagram of the proposed low pass filter.

The transfer function of the filter section is

$$A(S) = \frac{V_{in+}(S)}{V_{in}(S)} = \frac{1/R1C1}{S + 1/R1C1} = \frac{1}{1 + SR1C1} \quad (17)$$

The resistor R1 and capacitor C1 forms frequency circuitry for the said low pass filter.

Where the complex frequency variable, $s = \sigma + j\omega$ allows for any time variable signals. For pure sine waves, the damping constant, σ becomes zero and $s = j\omega$. For a normalized presentation of the transfer function, s is referred to the filter's corner frequency, or -3 dB frequency, ω_c in rad/sec, and has these relationships:

$$S = \frac{s}{\omega_c} = \frac{j\omega}{\omega_c} = \frac{jf}{f_c} \quad (18)$$

The magnitude of the gain response is:

$$|A(\omega)| = \frac{1}{\sqrt{1 + \left(\frac{\omega}{\omega_c}\right)^2}} \quad (19)$$

At $\omega = \omega_c$ the magnitude of the gain is 0.707 or -3 dB. Hence, the pass band is: $0 \leq \omega \leq \omega_c$, and the stop band is:

$\omega > \omega_c$.

We have $\omega_c = 1/R1C1$. The roll off factor for 1st order LPF is -20 dB/decade. The phase angle of the sinusoidal transfer function of the 1st order LPF is formulated as follows.

$$\angle A(\omega) = -\tan^{-1}(\omega R1C1) \quad (20)$$

At $\omega=\omega_c$, the phase angle becomes (-45°) and as frequency (ω) tends to infinity, the phase angle tends to (-90°) which concludes that the order of the filter is 1.

Results of Software simulation.

The working of the proposed circuit has been verified using cadence virtuoso simulation. The PMOS and NMOS transistors have been simulated by respectively using the parameters of a 0.13um tsmc13rf CMOS technology. The aspect ratios of PMOS and NMOS transistors are $W/L=(2u/300n)$, $(2u/350n)$ dimensionally respectively. First we investigated different parameters of NMOS OTA and CMOS OTA as defined below and their measured values are listed in Table I. Here we have set, $V_{dd}=3.3V$, $C_{load}=1nF$ for all the circuits and tuned ISS to get positive output voltage. In this section first order low pass filter using the proposed OTA is implemented with the power dissipation is 2.409mW.

The calculations are done according to the following definitions of the parameters:

- 1) Output Offset Voltage (V_{of}) is the output voltage, V_{out} with $V_{in+}=V_{in-}=0V$.

The output offset voltage is the voltage which appears at the output of the differential amplifier when the input terminals are connected together.

- 2) $CMRR (dB) = 20\log\left(\frac{A_d}{A_{cm}}\right) \quad (21)$

where, A_d =Differential Voltage gain and A_{cm} =Common mode voltage gain.

- 3) $PSRR(dB) = 20\log\left|\frac{\frac{V_o}{V_{id}(v_{dd}=0)}}{\frac{V_o}{V_{dd}(v_{id}=0)}}\right| \quad (22)$

- 4) Slew Rate (SR)= $\frac{\Delta V}{\Delta t}$ It is the maximum slope of the output voltage. The positive slew rate can be different from the negative slew rate.

For $V_{in+}=u(t)$, unit step signal with $V_{in-}=0V$.

- 5) Power dissipation: It depends on speed and bandwidth requirements.

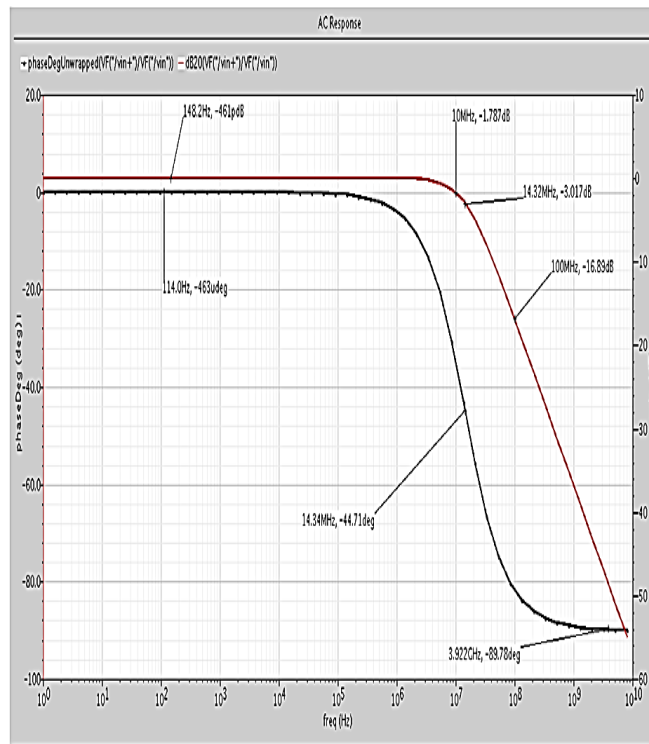


Fig. 23. Gain (db) and Phase angle (degree) vs frequency (Hz) plot of a 1st order LPF using NMOS OTA with simple current mirror load.

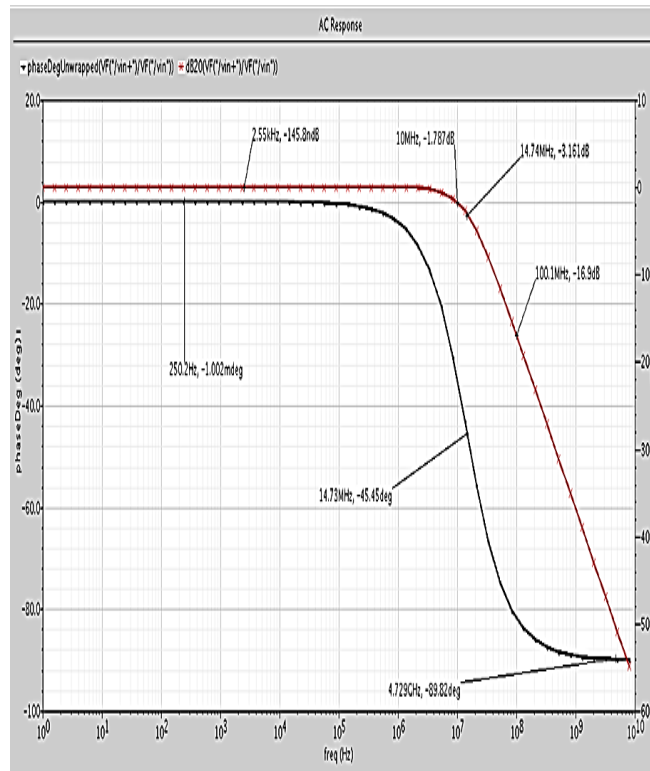


Fig .24. Gain (db) and Phase angle (degree) vs. frequency (Hz) plot of a 1st order LPF using NMOS OTA with Wilson current mirror load.

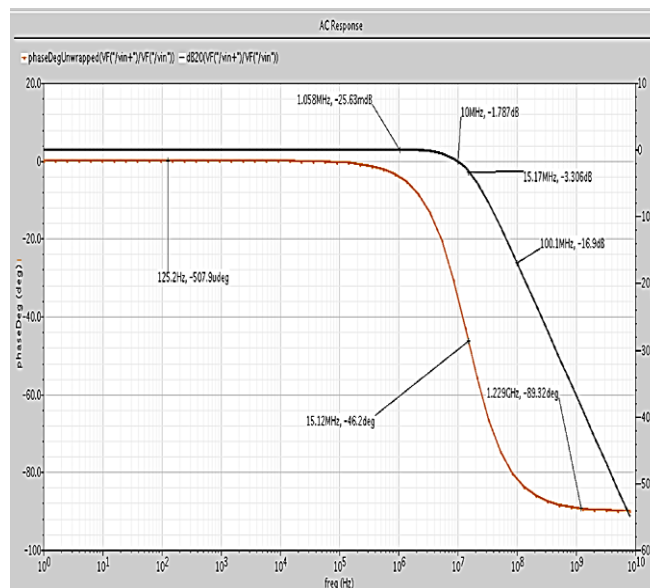


Fig .25 Gain (db) and Phase angle (degree) vs. frequency (Hz) plot of a 1st order LPF using NMOS OTA with cascode current mirror load.

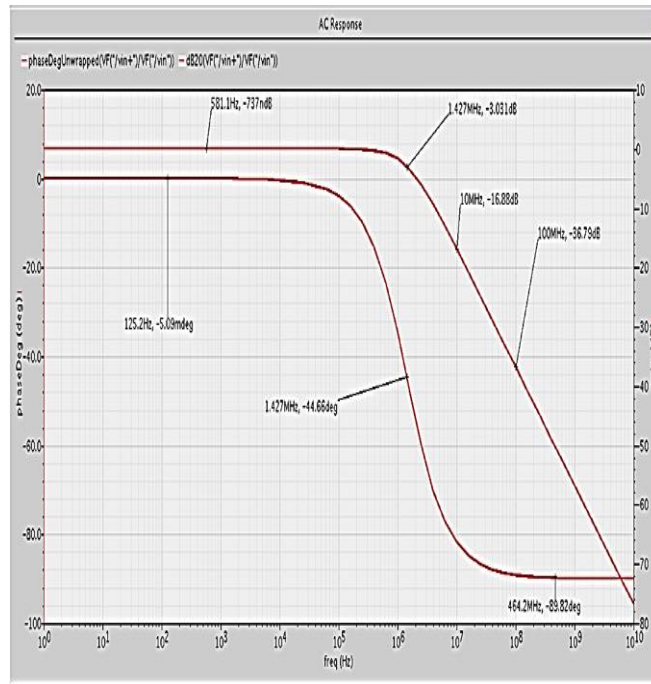


Fig. 26 Gain (db) and Phase angle (degree) vs frequency (Hz) plot of a 1st order LPF using CMOS OTA with simple current mirror load.

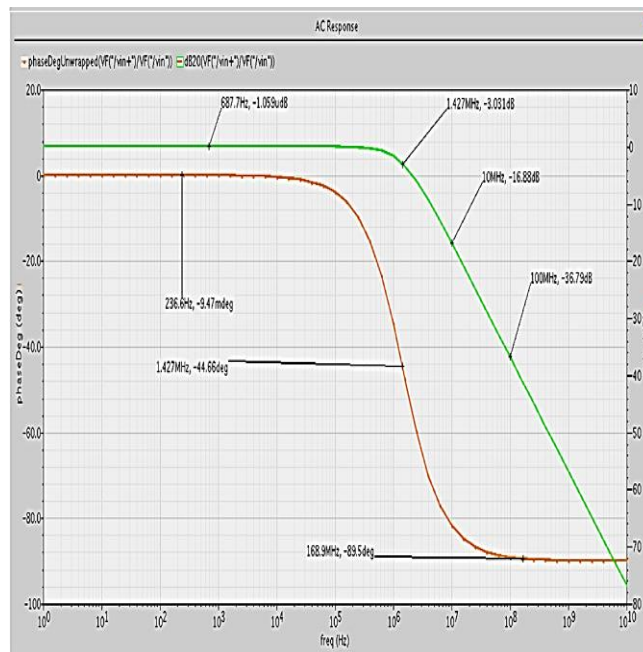


Fig. 27 Gain (db) and Phase angle (degree) vs frequency (Hz) plot of a 1st order LPF using CMOS OTA with willson current mirror load.

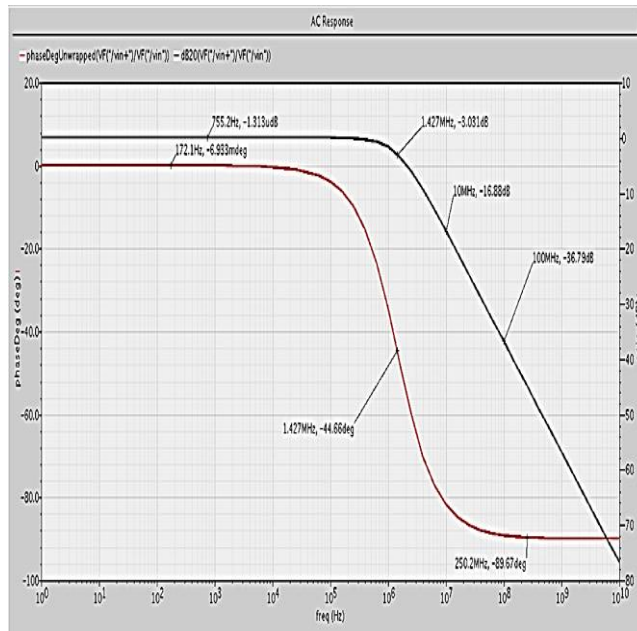


Fig .28 Gain (db) and Phase angle (degree) vs. frequency (Hz) plot of a 1st order LPF using CMOS OTA with cascode current mirror load.

Fig. 23-25 show the gain (dB) vs. frequency (Hz) and phase angle (degree) vs. frequency (Hz) plots for 1st low pass filter designed by NMOS and Fig. 26- 28 those for CMOS OTA with different current mirror loads as discussed earlier. For the design we have chosen $R1=0.110k\Omega$ and $C1=1nF$, $V_{in}=666mV$. The theoretical value of high cut-off frequency, $f_H = 1/2\pi.R1.C1=1.447kHz$. We assume the pass band gain as unity. In Fig. 23 the maximum pass band gain in dB, high cut-off frequency and its corresponding gain in dB are indicated. In Fig. 23 the phase angle at high cut-off frequency and also that as frequency tends to infinity are indicated. In Table I a parameter values of NMOs OTA and CMOS OTA are listed. In Table II all the specifications of the designed low pass filter are listed for all the circuits. In Table III the static power dissipations for all the circuits are listed.

Table I. Parameters of NMOS OTA and CMOS OTA.

Type of OTA	Type of current mirror load	Output offset voltage (V)	CMRR (dB)	PSRR (dB)	Slew Rate (V/ μ s)	Bias Voltage (V _{dd}) (Volts)	Sink Current (ISS)
CMOS	Cascode	-116.425 m	32.12	55.189	0.013	3.3	255uA
	Wilson	-1.12475	10.317	34.09	247.5	3.3	155uA
	simple	-1.94386	10.48480	38.9866	9.57142	3.3	2290uA
NMOS	simple	2.82317	3.7413	17.0994	0.00011636 36	3.3	5.9mA
	Wilson	-1.50864	-15.0518	43.8932	0.0002941	3.3	1.51mA
	Cascode	-1.36218	-13.9880	47.0803	0.00001248	3.3	1.4mA

Table II. All the specifications of the designed low pass filter.

Type of OTA	Type of current mirror load	High cut-off frequency (f _H) (kHz)	Maximum pass-band gain (dB)	Slope of the magnitude plot (dB/Decade)	Phase angle at f _H (degree)	Phase angle as frequency tends to infinity (degree)
NMOS	Cascode	15170	-0.2563	-15.1	-46.2	-89.32
	Wilson	14740	-145.8n	-15.13	-45.45	-89.82
	Simple	14320	-461p	-15.11	-44.71	-89.78
CMOS	Simple	14270	-737n	-19.91	-44.66	-89.82
	Wilson	14270	-1.06u	-19.91	-44.66	-89.5
	Cascode	14270	-1.313u	-19.91	-44.66	-89.67

Table III. Static power dissipation.

Type of OTA	Type of current mirror load	Bias voltage, V _{dd} (Volts)	Sink Current ISS	Static Power Dissipation
NMOS	Cascode	3.3	730 uA	2.409 mw
	Wilson	3.3	5020 uA	16.566 mw
	Simple	3.3	5490 uA	18.117 mw
CMOS	Simple	3.3	1670 uA	5.511 mw
	Wilson	3.3	940 uA	3.102 mw
	Cascode	3.3	170 uA	0.561 mw

Thus, by analyzing all the parameters for different configurations of the current mirror circuit we can conclude that the CMOS OTA using Cascode Current mirror circuit offers best performance and is suitable for operations required for the intention of our project, which is to design a LPF using CMOS OTA.

Applications of OTA based LPF.

After broad study, of all the choices Operational Trans conductor Amplifier is preferred to design a Chebyshev filter. Amongst all the architecture of OTA, on the basis of literature survey, Telescopic OTA is preferred as it has high gain, high speed low noise and low power consumption. The design procedure for a single stage telescopic OTA is designed using design equations. The circuit implemented is then simulated on Tanner EDA tool. The simulated results are validating the theoretical values.

E. Frequency response

Simple filters are usually defined by their responses to the individual frequency components that constitute the input signal. There are three different types of responses. A filter's response to different frequencies is characterized as pass band, transition band or stop band. The pass band

response is the filter's effect on frequency components that are passed through (mostly) unchanged. In fig.29, which shows the frequency response of a low pass filter, ω_p is the pass band ending frequency, ω_s is the stop band beginning frequency, and A_s is the amount of attenuation in the stop band. Frequencies between ω_p and ω_s fall within the transition band and are attenuated to some lesser degree.

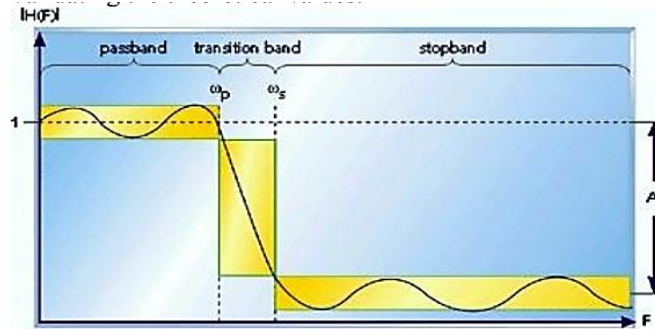


Fig.29. Response of a low pass filter to various input frequencies (Veeravalli, Sanchez-Sinencio and SilvaMartinez, 2002).

F. Chebyshev filters

Chebyshev (equal ripple magnitude). (Also, transliterated Tschebychev, Tschebyscheff or Tchevysheff.) This filter type has steeper attenuation above the cutoff frequency than Butterworth. This advantage comes at the penalty of amplitude variation (ripple) in the pass-band. Unlike Butterworth and Bessel responses, which have 3dB attenuation at the cutoff frequency, Chebyshev cutoff frequency is defined as the frequency at which the response falls below the ripple band. For even-order filters, all ripple is above the 0dB-gain DC response, so cutoff is at 0dB—see Fig.30. For odd -order filters, all ripple is below the 0dB-gain DC response, so cutoff is at $-(\text{ripple})$ dB—see Figure .31. For a given number of poles, a steeper cutoff can be achieved by allowing more pass-band ripple. The Chebyshev has even more ringing in its pulse response than the Butterworth.

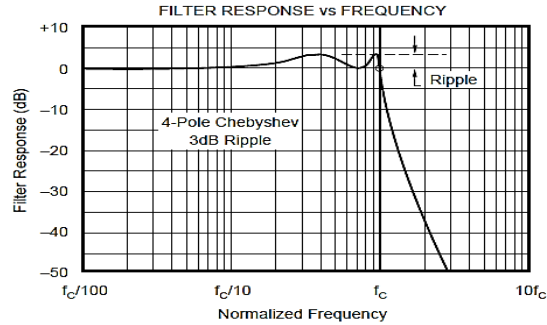


Fig .30 Response Vs Frequency of Even-Order (4-pole), 3dB Ripple Chebyshev Filter Showing Cutoff at 0dB.

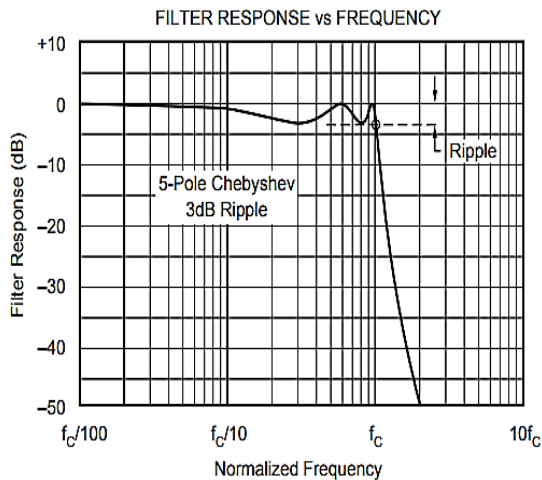


Fig .31. Response Vs Frequency of Odd-Order (5-pole), 3dB Ripple Chebyshev Filter Showing Cutoff at -3dB.

The word Chebyshev is known to a kind of filter response, not a type of filter. Chebyshev filters have the feature that they diminish the error between the idealized filter characteristic and the definite over the range of the filter, but with ripples in the passband. As the ripple increases (bad), the roll-off tends sharper (good). The response of Chebyshev filters is based on the minimization of the maximum error in the complete passband, significant in passband ripples with equal amplitude. The larger the ripple amplitude accepted, the steeper the transition roll-off. Chebyshev filters are also well-known as “quirpele” or “minimax” filters due to their features. The Chebyshev lowpass magnitude response can be described by:

$$|H(\omega)|^2 = \frac{1}{1 + \varepsilon^2 T_n^2\left(\frac{\omega}{\omega_p}\right)} \quad (23)$$

$$T_n(x) = \begin{cases} \cos(n \cos^{-1} x) & ; \quad |x| \leq 1 \\ \cosh(n \cosh^{-1} x) & ; \quad |x| > 1 \end{cases} \quad (24)$$

The magnitude of $T_n(x)$ oscillates between ± 1 for $|x| \leq 1$ and grows as n^x for $|x| > 1$. If ε is passband ripple, “A” is the stopband attenuation, ω_p is passband edge frequency and ω_s is the stopband edge frequency, then the required filter order can be determined as:

$$n = \frac{n \cosh^{-1} \sqrt{1 - \frac{1}{\varepsilon}}}{n \cosh^{-1}\left(\frac{\omega_s}{\omega_p}\right)} \quad (25)$$

G. Chebyshev

- Advantages: Better attenuation beyond the pass-band than Butterworth.
- Disadvantages: Ripple in pass-band. Considerable ringing in step response.

Table IV shows comparison results about the performance of proposed OTA CMOS with (Carrillo, and Torelli, 2008; Pan, et al. 2009; Chatterjee, Tsvividis, and Kinget, 2005) but in Table V shows Comparison of Proposed Filter OTA CMOS with the previous (Lee, et al. 2009; Soliman, et al. 2013)

Table IV. Comparisons of characteristics of proposed OTA with other.

	Ref (15)	Ref (16)	Ref (17)	Ref (18)	Proposed OTA CMOS		
					simple	cascode	Wilson
Supply (V)	0.8	0.9	0.5	1	3.3	3.3	3.3
CMRR (dB) @5kHz	100	129	78	--	10.48480	32.12	10.317
+PSRR (dB)	-	-	-	-	38.98666	55.189	34.09
SR (V/ μ s)	-	-	-	-	9.57142	0.013	247.5
Power dissipation (mW)	0.1	0.0099	0.1	0.0443	5.511	0.561	3.102
Tech	0.18	0.35	0.18	0.35	0.13	0.13	0.13

Table V. Comparison of proposed filter with the previous

Parameters	2009 Ref (19)	2013 Ref (20)	Proposed Filter with OTA CMOS		
			simple	cascode	Wilson
Supply (V)	± 1	± 0.8	3.3	3.3	3.3
V _{th}	0.5V	0.53V	0.654V	0.654V	0.654V
Order	5	5	1	1	1
Bandwidth	250hz	243hz	14270K hz	14270K hz	14270K hz
Tech	180nm	250nm	130 nm	130 nm	130nm

CONCLUSIONS.

The Operational Transconductance amplifiers are important building blocks for various analog circuits and systems which were previously implemented by using OPAMP. Currently, research is on for implementation of OTA circuits that will be highly linear, consume less amount of power and operate at low power supply. Processing of a signal is not possible without filters. From the above design of 1st order LP filter we can analyze that cascading of filters leads to the higher order filter with reduced transition band. On increasing order of the filter transition band can be reduced but it may lead to unstable the system due to large number of capacitors. We call our proposed OTA based LPF as tunable because by adjusting the values of power supply and sink current we can get different pass band gain less than unity. Again, the high cut-off frequency can be adjusted by changing simply the values of resistor, R and capacitor, C of the input RC section. The other advantages of our design over conventional OPAMP based LPF are (1) a single power supply is required, (2) CMRR, PSRR, slew rate are better. (3) noise margin is high, (4) design is very simple, (5) fabrication cost is reduced greatly.

BIBLIOGRAPHIC REFERENCES.

1. Acosta, L. Mariano Jiménez, Ramón G. Carvajal, G. (2009). Highly Linear Tunable CMOS Gm-C Low-Pass Filter(J). IEEE Transactions on circuits and systems:2145-2158.
2. Carrillo, J.F. and Torelli, G. (2008). "1-V continuously tunable CMOS bulk-driven transconductor for Gm-C filters," 2008 IEEE International Symposium on Circuits and Systems, pp. 896-899, 2008.
3. Chatterjee, Y. Tsvividis, and P. Kinget, (2005). 0.5-V analog circuit techniques and their application in OTA and filter design. IEEE Journal of Solid- State Circuits. 40(12), pp. 2373-2387.
4. Geiger, D. and Sánchez-Sinencio, E. (1985). "Active filter design using operational transconductance amplifiers:A tutorial," IEEE Circuits and Devices Magazine, vol. 1, pp. 20-32, Mar. 1985.
5. Hsu, M. Ho, K. Wu, T. and Chen, H. (2006). "Design of low-frequency low-pass filters for biomedical applications," in Proc. IEEE Asia Pacific Conference on Circuits and Systems, Dec. 2006, pp. 690-695.
6. Lee, G. Member, D. And Chih-Jen, C. (2009). "Systematic Design and Modeling Of A Ota-C Filter For Portable Ecg Detection", IEEE Transactions On Biomedical Circuits And Systems, Vol. 3, No. 1, pp.53-64.
7. Liu, X. Peng, and W. Wu, (2009). "Design of a Gm-C low pass filter with low cutoff frequency," in Proc. Asia Pacific Conference on Postgraduate Research in Microelectronics and Electronics, pp. 125-128.
8. Mahapatra, M. Singh, and N. Kumar, (2009). "Realization of active filters using operational transconductance amplifier (OTA)," Journal of the Instrument Society of India, vol. 35, no. 1, pp 1-9.

9. Malvar, H. (1982). "Electronically controlled active filters with operational transconductance amplifier," *IEEE Transactions on Circuits and Systems*, vol. CAS 29, pp. 333-336.
10. Pan, D. Chiung-Cheng, C. Chung-Huang, Y. Yu- Sheng, L. (2009). A Novel OTA with Dual Bulk-Driven Input Stage, pp. 2721-2724.
11. Salman, M. A., & Borkar, V. C. (2016). New Method to Calculate the Matrix Exponential. *International Journal of Engineering, Science and Mathematics*, 5(1), 210-218.
12. Soliman A. Mahmoud, N. Ahmed, B. Saeed A. Al-Tunaiji, F. (2013). "Low-Noise Low-Pass Filter For Ecg Portable Detection Systems With Digitally Programmable Range", *Circuits Syst Signal Process*, Vol 32, pp.2029–2045.
13. Solis-Bustos, J. S. Martinez, F. Maloberti, and Sanchez-Sinencio, E. (2000). "A 60-dB dynamic-range CMOS sixth-order 2.4-Hz low-pass filter for medical applications," *IEEE Transactions on Circuits and Systems*, vol. 47, no. 12, pp. 1391-1398, Dec. 2000.
14. Timar, F and Rencz, M. (2007). "Design issues of a low frequency low-pass filter for medical applications using CMOS technology," in *Proc. IEEE Design and Diagnostics of Electronic Circuits and Systems*, pp. 1-4.
15. Veeravalli, E. Sanchez-Sinencio, D and SilvaMartinez, J. (2002). "Transconductance amplifier structures with very small transconductances:A comparative design approach," *IEEE J. Solid State Circuits*, vol. 37, no. 6, pp. 770–775.
16. Villegas, A. Casson, J. and Corbishley, P. (2011). "A subhertz nanopower low-pass filter," *IEEE Transactions on Circuits and Systems II*, vol. 58, no. 6, pp. 351-355.
17. Waldman, A. García, D. González, G. and Cordero. O. (2018). "Factores que determinan la selección de la universidad destino en el ámbito internacional." *Opción* 34.86: 235-258.

DATA OF THE AUTHORS.

1. Ridouane Hamdaouy. University Sidi Mohamed Ben Abdellah, LESSI Laboratory, Department of Physics Faculty of Sciences, Dhar El Mehrez B.P. 1796, 30003 Fez-Atlas, Morocco. Email:

ridouane.hamdaouy@usmba.ac.ma

2. Mostapha Boussetta. University Sidi Mohamed Ben Abdellah, LESSI Laboratory, Department of Physics Faculty of Sciences, Dhar El Mehrez B.P. 1796, 30003 Fez-Atlas, Morocco. Email:

mostapha.boussetta@usmba.ac.ma

3. Khadija Slaoui. University Sidi Mohamed Ben Abdellah, LESSI Laboratory, Department of Physics Faculty of Sciences, Dhar El Mehrez B.P. 1796, 30003 Fez-Atlas, Morocco. Email:

slaoui.khadija@usmba.ac.ma

RECIBIDO: 2 de febrero del 2019.

APROBADO: 10 de febrero del 2019.